ate prototypes and models (toys). However, this is sufficient and adequate for the purposes of this sector (design patterns, rapid visualization of new ideas).

Because of substantial advancements in all the technologies mentioned, newly developed methods such as SHS, AKF, and MFJ, and future changes in the characteristics that are not to be excluded, the characteristics of Table 1.1 require constant re-evaluation.

1.2.4 Laser Sintering (LS)

AM-components made as described in Table 1.1, rated by industry standard criteria such as mechanical properties, thermal stability, component precision, surface quality, and long-term stability, as well as a few others, should meet the demand in terms of the production of functional parts. Essentially, only laser sintering is qualified nowadays. The cohesion of the building materials is carried out by a thermal process that includes the melting of the powder followed by solidifying it into the desired shape.

The LS process is currently considered as the AM process that will be able in the future to permanently cross the border between prototyping and functional components. This step is considerable because it means that the technology must meet completely different requirements in terms of reproducible quality, process reliability, automation of production processes, and other production-typical requirements.

The step from prototype to production part changes the perspective entirely. Both LS parts and the LS process have to be measured in the context of traditional and established production technologies. Only by succeeding at this step can a wide industry acceptance be expected in the future. For this, all levels of the LS process chain must be considered. Figure 1.4 shows schematically the factors that influence the LS process.
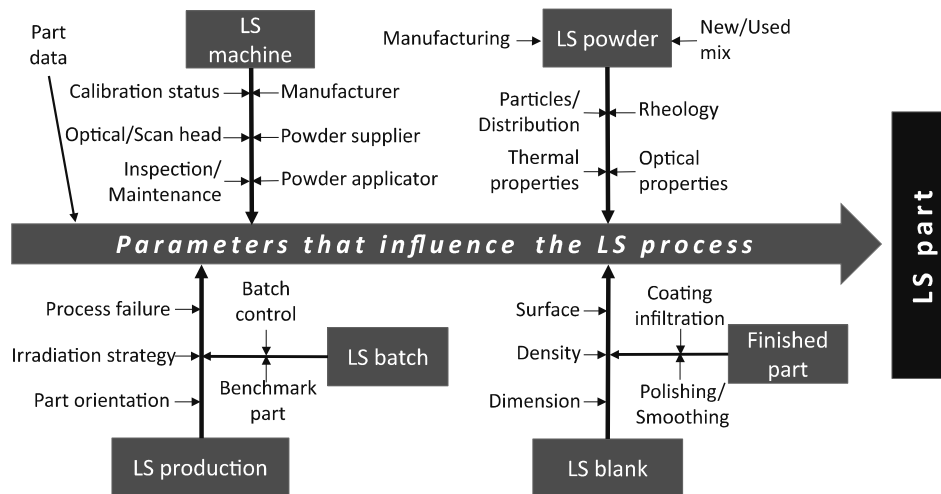
Figure 1.4 Process chain and influences on additive manufacturing with LS

All areas featured in Figure 1.4 are addressed in this book and discussed in detail:

LS technology (Chapter 2): This section describes the machine technology of the current LS devices and adds special emphasis on where the technologies of individual manufacturers differ and the resulting effects. Temperature control, powder feed, energy input, and optical components are the focus. A summary of the equipment currently available in the market completes the differentiation.

LS process (Chapter 3): This section explains key process details before and during the fabrication process. The powder preparation, the process flow, and process errors are discussed. Opportunities for quality control throughout the supply chain and the level of international standardization are presented.

LS materials: Another priority of this book is the polymeric materials that can be processed by LS technology **(Chapter 6 – LS materials: Commercial materials)**. First, the question of the specific requirements imposed on the plastics to make them accessible to the LS process is presented **(Chapter 4 – LS materials: Polymer properties)**. In Chapter 5, special attention is placed on the preparation of suitable polymer powders and the evaluation of their properties **(Chapter 5 – LS materials: Polymer powder)**.

LS parts (Chapter 7): In the final chapter, the mechanical properties and the density of LS parts are finally addressed. Some selected examples of parts are also illustrated, including the design features and the limitations of the LS method, as well as the specific advantages that LS parts can have compared to plastic parts that have been produced with other plastics processing methods (e. g., injection molding).

■ 2.1 Machine Technology

2.1.1 Machine Configuration

The market-leader systems from 3D Systems and EOS are structurally similar at their core but differ in details such as powder feed, powder application, optical correction, and the irradiation strategy.

The basic structure of an LS machine consists of three levels, as shown in Figure 2.3: optics module, build chamber with build area, and powder area.
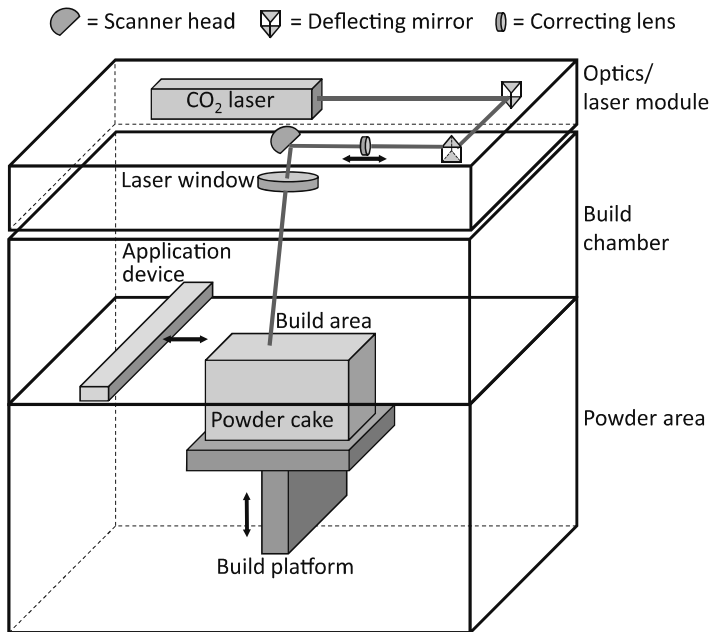

Figure 2.3 Basic structure of an LS machine

The optics, or laser, module contains the laser, the beam path with the corresponding deflecting mirrors, a correcting lens for focus adjustment, and the scanner head. This machine component is hermetically sealed from the rest of the machine and must be dust-free. Dust particles on the optical elements would lead to dispersion losses of the laser radiation and a massive negative impact on the quality of the parts built by the process.

Figure 2.4 shows a view of the laser module of a DTM Sinterstation 2500plus. The laser, the deflecting mirrors, the correcting lens, and the scanning head are clearly visible. Not depicted here are the electronic control modules of the scan head, which are also housed in a dust-free environment in the laser module area.
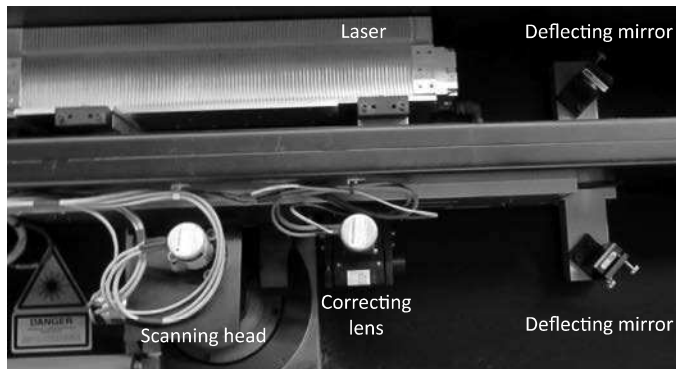
Figure 2.4 Top view of the laser module of an LS machine: the laser, the deflecting mirrors, the correcting lens, and the scanning head are visible [source: Inspire AG]

Under the scanning head in Figure 2.4, the laser window can be seen, which represents the interface to the underlying build area. The laser window consists of special optical materials with an extremely high transmission for the corresponding laser wavelength. In the case of LS machines with a CO_2 laser (λ = 10.6 µm), zinc selenide (ZnSe) is used for the laser window. Figure 2.5 shows the components of the laser window when it is installed and uninstalled.
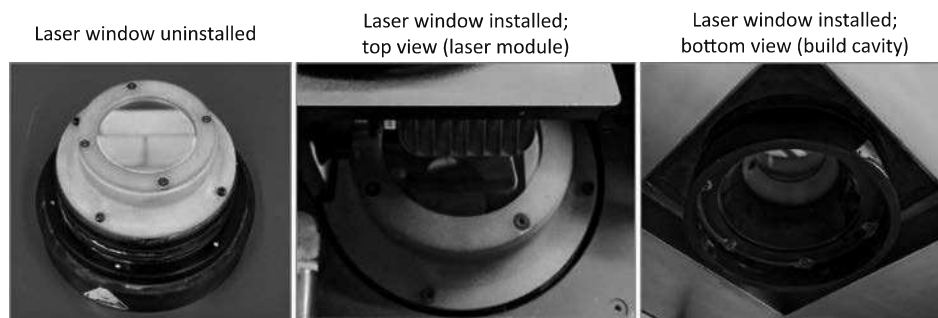
Figure 2.5 Laser window installed and uninstalled [source: Inspire AG]

For a good sintering result, the laser window should/must be cleaned carefully after each LS build. Deposits or burnt particles would massively affect the process. The laser window must be replaced periodically due to wear, since it can become "blind" over the course of many build cycles.

The next two areas in an LS machine are the build chamber and the powder area. These two regions are connected to each other through the build area. In the case of DTM/3D Systems technology, the powder feed takes place (see Section 2.1.3.1) at the interface between build and powder area, that is, the storage for the powder is located in the powder area.

Ideally, all the parts at the end of the entire build process are in good shape, as shown in Figure 3.11. No part distortion or other process errors can be seen there.

3.1.4 Process Errors

As with other manufacturing processes, a whole range of process issues can occur in the LS process. These result in either rejected parts or, in the worst case, a termination of the build process with damage to the machine components (see Figure 3.12, left).
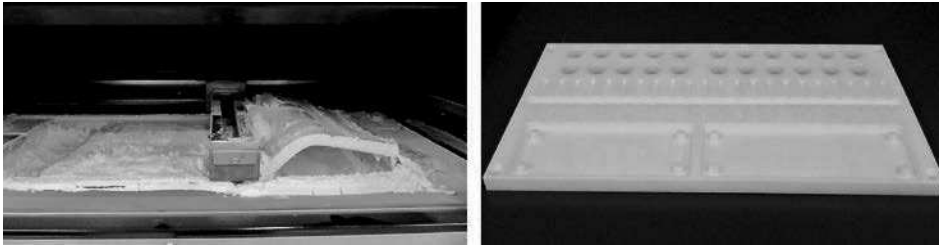
Figure 3.12 Build termination due to blocking of the coating unit [source: Inspire AG]

During the production of the large part with flat areas shown in Figure 3.12 (right side), the incorrect positioning of the part caused a massive overheating of individual layers, which resulted in a partial melt of the build area. Thus, the coater has collected the already sintered layers and moved them aside. The complete build had to be rejected, and the coating unit had to be completely re-adjusted.

Problems are not always as massive as shown in Figure 3.12. In many cases, the entire build job is finished easily and problems are only detected when the parts are unpacked, showing part distortion or other geometrical deviations (deformations).

3.1.4.1 Deformation of the Part

The deformation of the parts occurs in different stages of the process: during the build phase (in build) or after the build phase (post build). Usually it is referred to as "curling" when the first sintered layers of the part are directly affected from distortion and the rest of the layers were built geometrically correct. In the case of "warpage", the parts have been built properly and twisted after finishing (e. g., wrong cool down). In Figure 3.13, the differences are shown schematically.
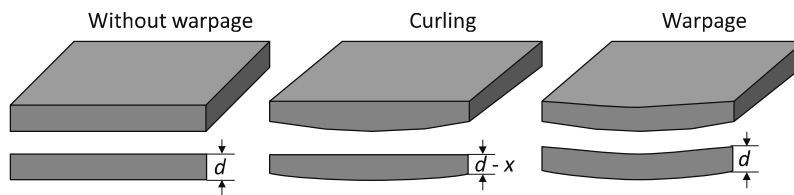
Figure 3.13 Differences in part distortion: curling and warpage

Curling can occur during the process in such a severe manner that the build process must be stopped immediately. Figure 3.14 shows an example of a massive curling effect, which led to the termination of the build process. If the edges of the parts, as shown in Figure 3.14, are already so protruded from the powder bed in the first layers, the roller would displace the part and destroy the powder bed at the next powder application by the roller.

Figure 3.14 Massive curling in the first layers of the part [source: Inspire AG]

Part warpage can also be triggered by incorrect part positioning in the build area. Figure 3.15 shows a typical case. Eight very thin but large components should be produced, for cost reasons, in a single build. For this, six parts are positioned flat and two parts are in the perpendicular position in the build job (Figure 3.15, right). While the six parts built horizontally (XY positioning) have predominantly straight walls and minimal warpage, the two left and right standing parts are highly warped and useless (see Figure 3.15, left).

In addition to the above different warpage types, there are other process errors that generate surfaces problems, which, due to their wavy appearance, are likened to an orange peel.
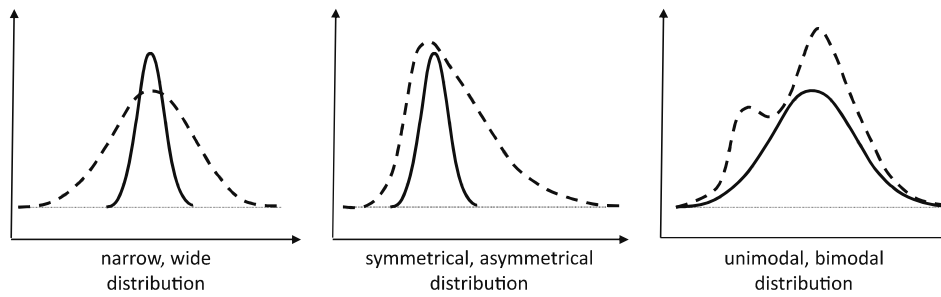
Figure 4.23 Some possible basic powder distributions

The distribution of the powder sizes has, like the powder geometry and especially the particle shape, an impact on the part packing density of the powder in the LS build cavity. Which is the best or most favorable distribution for the LS process cannot be assessed spontaneously. With regard to the powder density, a high part packing density of the particles is certainly desirable.

4.2.4.3 Powder Density

The density of powder particles can achieve a theoretical maximum value of 74% space filling in a cubic face-centered structure. This is strictly true only for unimodal distributed powders whose particles are ideally spherical. With the addition of smaller particles, which can fill the cavities between the large spheres, theoretically the maximum density can still be increased by a few percent [17].

However, it should be noted that, in reality, the theoretical density value and further optimization by mixing different fractions of powder are hardly practical. On the one hand, there are usually no ideally spherical, unimodally distributed powders of any size that can be mixed together. On the other hand, at non-ideal mixing ratios, the smaller particles in the powder are placed in such a way that the distance between the large particles increases again, and thus the density is reduced (an increase in the specific volume of the system).

Figure 4.24 shows the relationship schematically. Different bimodal mixtures can be produced from two ideal powders of different sizes. Only when the small particles exclusively occupy the cavities between the large particles is there a (slight) increase in the powder density. If the mixing ratio is not ideal, the powder density will decrease.

In addition, in mechanical loads, such as mixing processes, there is always a counter-effect. Fine powder separates from the large particles, floating up (shaking effect), so mixing and demixing compete.
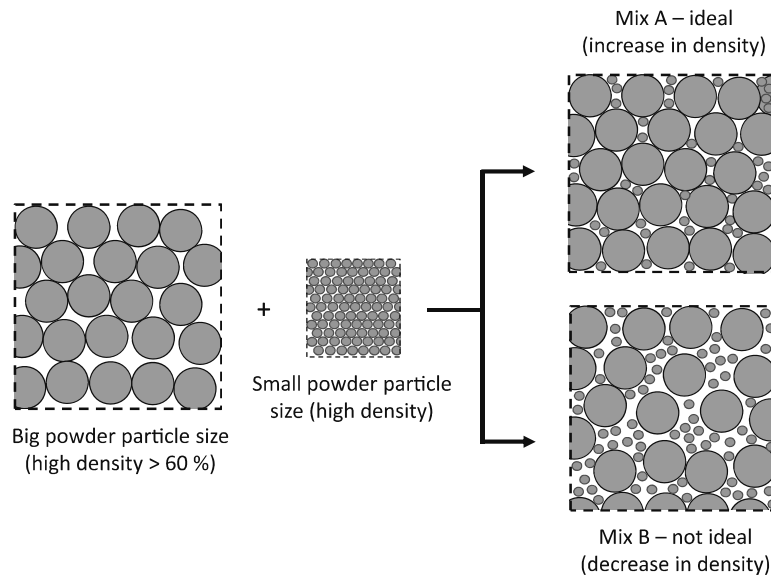
Figure 4.24 Part packing density of ideal spherical spheres in two sizes and bimodal mixtures

The part packing density of powders in technical applications achieves a maximum value of approximately 60%. For this purpose, nearly spherical particles are also required. The geometric deviation of the particles from the ideal spherical shape causes the practicable part packing density to fall rapidly, so that, in the case of today's commercially available LS powders, a powder density in the range of 45 to 50% can be expected.

The relationship between particle shape and the magnitude of the powder density is shown schematically in Figure 4.25. A rapid drop in the powder density with the deviation of the particles from the ideal circularity can be seen.
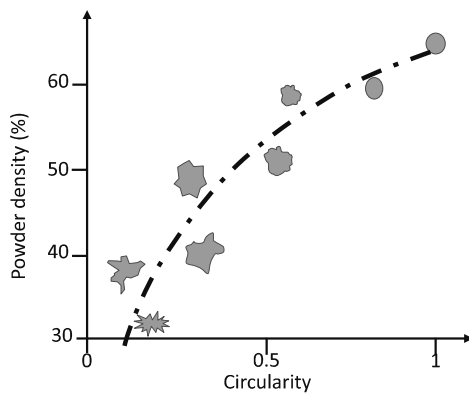
Figure 4.25 Relationship between particle geometry and powder density

If the powder density in the LS process is low due to, for example, a highly heterogeneous particle shape (often the case with grinded powders), only a small amount of material is deposited per volume fraction during powder application. After melting by the laser, the molten polymer flows together, and in the melt path of the laser, there is not enough material to generate homogeneous parts with sufficient structural integrity.

Figure 4.26 shows a part (the shoulder area of a DIN tensile bar) after a few sintered layers. In the left image, the sample was produced from powder with very low powder density, and, for comparison, a standard part (commercial PA 12 LS powder with sufficient density) is shown in the image on the right. As can be seen in Figure 4.26 (left side), the low powder density results in the formation of massive cavities and an uneven surface structure. The corresponding parts are unusable.

Sintered part with low
density powder

Sintered part with sufficient
density powder
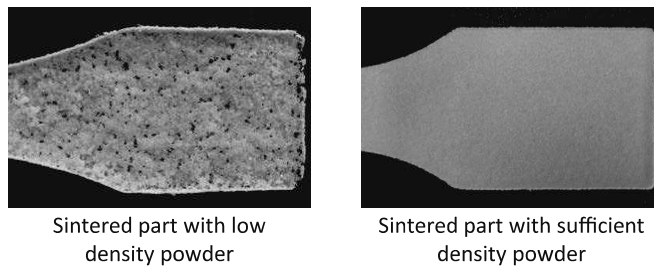
Figure 4.26 Test parts after a few sintered layers with different powder density
[source: Inspire AG]

From the explanations in Section 4.2.4, it becomes clear that the shape and the surface of the individual powder particles are of particular importance for the behavior of the corresponding powders in the LS process. Flowability and fluidization based on powder form, distribution, and density: these are decisive variables as to whether a powder can be successfully used and processed by LS or not.

The question of how the corresponding particles can be produced, from which promising LS powders can be generated, is therefore of central importance for future developments in this area (see Chapter 5).

■ 4.3 References of Chapter 4

[1]   Kaiser, W., *Kunststoffchemie für Ingenieure – Von der Synthese bis zur Anwendung*, Carl Hanser Verlag, 3rd Edition, Munich, ISBN: 978-3-446-43047-1, 2011

[2]   Osswald, T. A. and Menges, G., *Material Science of Polymers for Engineers*, Carl Hanser Verlag, 3rd Edition, Munich, ISBN 978-1-56990-514-2, 2012

6.1.3 Comparison of PA 12 and PA 11

The LS Rilsan® Invent materials are also adapted to the LS process with regard to their thermal properties, as described in Section 6.1.1.2 for the corresponding PA 12 materials. For example, Rilsan® Invent powder shows a relatively sharp melting peak at about 201 °C in the initial state, which is clearly above the melting point of standard PA 11 (about 186 °C). The effect of increasing the PA 11 sintering range by increasing the melting point ($\Delta T \approx 15$ °C) is therefore even more pronounced with Rilsan® Invent than with the corresponding PA 12 (Orgasol® Invent Smooth).

The production of Rilsan® Invent powder is carried out by means of a grinding process. In a further process step (annealing), the thermal properties are adapted for the LS process. The edges of the milled particles are also rounded in order to improve the flowability of the powders. Figure 6.17 shows the PA 11 particles (Rilsan® Invent) compared to Orgasol® Invent Smooth. The PA 11 particles exhibit an angular structure, as is typical for ground powders. The rounded edges are clearly visible. The powder distribution of Rilsan® Invent is significantly wider than that of PA 12 and has a d_{50} of approximately 50 μm (d_{50} (Orgasol® Invent Smooth) of approximately 43 μm).
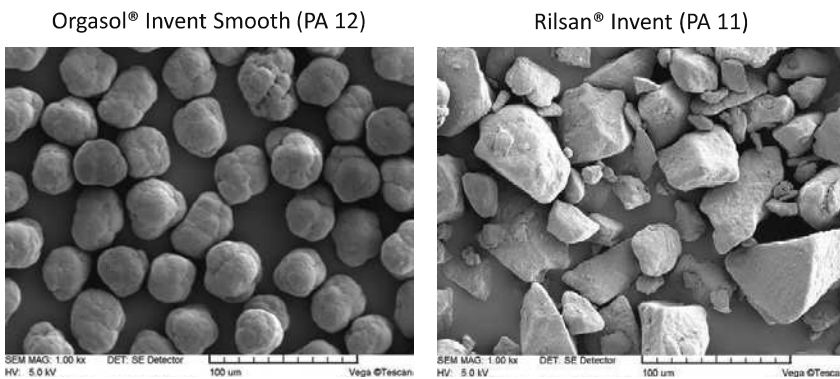
Figure 6.17 SEM images from Rilsan® Invent compared to Orgasol® Invent Smooth; particle form and shape as a result of different manufacturing processes [source: Empa]

Overall, the basic properties and basic data for PA 12 and PA 11 for LS use can be compared with each other as shown in Table 6.4. It should be noted that these are the values from the data sheets supplied by the material manufacturers and the information is valid for test specimens built in the *XYZ* direction (see Figure 7.5 in Section 7.1.1.5).

Table 6.4 Compilation of the Basic Data for Unreinforced Commercial PA 11 and PA 12 LS Materials (XYZ Build Direction)

Name	Elastic modulus (MPa)	Tensile strength (MPa)	Elongation at break (%)
PA 12 natural			
PA 2200/PA 2201/EOS (Germany)	1,700	48	15
Duraform® PA/3D Systems (USA)	1,586	43	14
Orgasol® Invent Smooth/Arkema (France)	1,800	45	20
PA 11 natural/black			
Rilsan® Invent/Arkema (France)	1,500	45	45

As already mentioned, the outstanding element for PA 11 is the significantly higher ductility of the materials compared with PA 12. This leads to a significantly higher elongation at break in the tensile test (about 45%) and also to an increased impact strength. The significantly improved toughness of the PA 11 materials is essentially based on the following molecular parameters:

- PA 11 thermally crystallizes exclusively in the α-triclinic form. This form is planar and requires no additional twisting of the amide units by 60°, such as the γ-monoclinic crystal structure (steric/kinetic hindrance).

- Due to the shorter PA 11 chains (a CH_2 unit less per molecular unit cell), PA 11 has more hydrogen bonds (HB) per polymer chain of the same length: PA 11 = 1 HB per 10 CH_2 groups, PA 12 = 1 HB per 11 CH_2 groups.

- Hydrogen bonds form a pronounced intramolecular cohesion and increase the melting point (odd-even effect [5]).

- In mechanical stress, the α-triclinic crystal lattice deforms better, and a transformation in a pseudohexagonal space lattice takes place. During this conversion, a considerable portion of the external load is absorbed (dissipated), which leads to a higher fracture energy absorption.

The cause for the higher ductility of PA 11 is therefore found in a combination of molecular material parameters. Specifically, the relatively higher number of hydrogen bonds and the ability to transform the crystal modification under stress are crucial.

In summary, the two currently most important materials for the LS process, PA 12 and PA 11, can be characterized and compared for the LS process as shown in Table 6.5.

Table 6.5 Basic Properties of PA 11 and PA 12 for LS Use

	PA 12	PA 11
Crystalline structure	γ-monoclinic	α-triclinic → pseudohexagonal
Sintering window	large	small to medium
Melting point (T_m)	182 to 186 °C	186 to 201 °C
Elastic modulus	approx. 1,700 MPa	approx. 1,500 MPa
Elongation at break (%)	15 to 20%	45%
Impact strength (charpy)	34 to 50 kJ/m^2	no break

The positive properties profile of PA 11, especially with respect to mechanical requirements, means that some compounds are also based on Rilsan® Invent for the LS application. As a result of the mixing with additives, the elongation at break generally decreases, which is somewhat compensated by the higher value for neat PA 11.

6.1.4 PA 12 and PA 11 Compounds

The commercial LS base powders presented in the previous sections serve as basic materials for a whole range of LS compound materials. However, it should be emphasized that these are not compounds such as in the injection molding field, but dry blends.

The base powder and the respective additive are thus only mixed mechanically (blended). Essentially, metal powders, some fiber grades, and glass spheres are mixed. Figure 6.18 shows the SEM images of two blends. On the left, a mixture of PA 12 powder with carbon fiber; on the right, the proportion of glass spheres (perfect spherical particles) is clearly visible alongside the powder particles.

Blend of LS PA 12 and carbon fiber　　　Blend of LS PA 12 and glass spheres
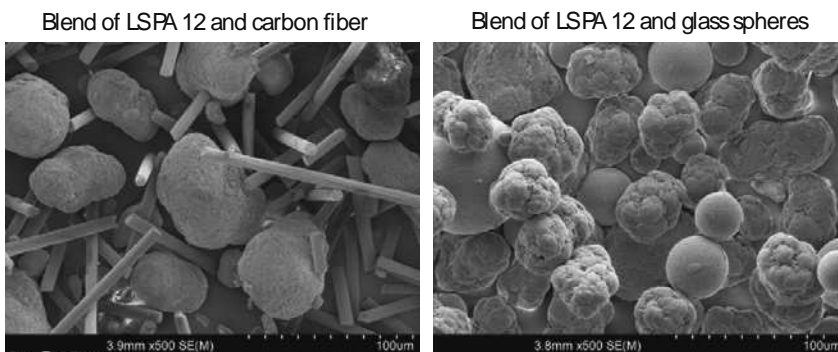
Figure 6.18 SEM image of PA 12 LS powder filled with carbon fibers or glass spheres [source: Empa]

Index